

Polyesters with dicyanovinyl group were newly prepared from **3** and common diols with terephthaloyl chloride. They showed an enhanced solubility in polar aprotic and common organic solvents.

The polymers showed two consecutive exotherms in DSC thermograms attributable to the chemical change of dicyanovinyl group along with decomposition.

They undergo a curing reaction at around 350 °C, and show a 50-60% of residual weight at 500 °C indicating that the thermal stabilities were enhanced.

### References

1. Spinelli, H. J.; Harris, F. W. Eds. *Reactive Oligomers*; ACS Symposium Series 282; American Chemical Society: Washington, DC, 1985; pp 1-115.
2. Cassidy, P. E. *Thermally stable polymers*; Marcel Dekker: New York, 1980
3. Moore, J. A.; Robello, D. R. *Macromolecules* **1986**, *19*,

- 2667.
4. Moore, J. A.; Robello, D. R. *Macromolecules* **1989**, *22*, 84.
5. Moore, J. A.; Mehta, P. G. *Polym. Mater. Sci. Eng.* **1990**, *63*, 351.
6. Moore, J. A.; Mehta, P. G. *Polym. Mater. Sci. Eng.* **1991**, *64*, 835.
7. Gong, M. S.; Moon, H. S.; Kim, S. T. *Makromol. Chem. Rapid Commun.* **1991**, *12*, 591.
8. Gong, M. S.; Moon, H. S.; Kim, J. S.; Kim, C. B. *Polym. J.* **1993**, *25*, 193.
9. Gong, M. S.; Choi, S. H.; Kim, S. T.; Kim, J. S. *Polym. J.* **1993**, *25*, 763.
10. Gong, M. S.; Moon, H. S.; Kim, S. T. *Macromolecules* **1992**, *25*, 7392.
11. Gong, M. S.; Kim, B. G.; Kim, Y. S. *Polym. J.* **1994**, *26*, 1910.
12. Gong, M. S.; Cho, H. G.; Kim, B. G.; Choi, S. H. *Macromolecules* **1993**, *26*, 6654.

## MO Calculation for the Dissociative Adsorption of Oxygen Molecule on Ni44(111) Model Surface

Kwang Soon Lee<sup>1</sup>, Hyun Joo Koo, and Woon Sun Ahn\*

*Department of Chemistry Sung Kyun Kwan University, Suwon 440-746, Korea*

<sup>1</sup>*Department of Chemistry, Song Sim University, Puchon 422-743, Korea*

*Received August 17, 1994*

The interaction of oxygen molecule with Ni44(111) model surface to which the molecule approaches is studied by calculating the relevant DOS and COOP with the tight-binding EHT method. It is found that the dissociative adsorption of oxygen takes place as a result of electron transfer from the Ni *dn* orbital to the antibonding 1 $\pi_g$  orbital of the oxygen molecule. This finding is noteworthy to contrast with the case of Ni(100) surface in which the electron transfer takes place from the Ni *d<sub>z<sup>2</sup></sub>* orbital of the nickel surface.

### Introduction

It is widely accepted that oxygen is dissociatively adsorbed on nickel metal surface via molecular precursor state. Shyegan *et al.*<sup>1</sup> studied the work function of Ni(111) surface at 5.5 K with varying degrees of oxygen coverage, and reported the existence of molecular oxygen which might be the precursor species to the dissociatively adsorbed oxygen. The life-time of this molecular precursor is so short that it can hardly be detected. Ahn *et al.*<sup>2</sup> showed an evidence of the molecular precursor state by calculating the activation energy of the dissociative adsorption of oxygen molecule on a polycrystalline nickel surface by means of the X-ray photoelectron spectroscopy. Beckerle *et al.*,<sup>3</sup> on the other hand, reported that they were unable to find an evidence of the molecular state precursor at 8 K from EELS and work function measurements.

The experimental studies with LEED,<sup>4,5</sup> AES,<sup>6-8</sup> XPS<sup>9,10</sup> and many other surface analyzing techniques show that the

dissociatively adsorbed oxygen atoms on the nickel surfaces form p(2×2) structure initially. This structure changes to c(2×2) structure followed by NiO formation with increasing oxygen adsorption.<sup>4,6,11,12</sup> Ahn *et al.*<sup>13</sup> observed that the dissociatively adsorbed oxygen atoms on polycrystalline nickel surface show several different degrees of oxidation from the XPS measurements at the temperature ranges from 300 K through 500 K. Marcus *et al.*<sup>14</sup> investigated the p(2×2) oxygen layer on a Ni(111) plane with LEED spectroscopy and concluded that the oxygen atoms occupy the three-fold centre of the nickel surface with the Ni-O distance of 19.4 nm.

Hoffmann *et al.*<sup>15-17</sup> introduced the Hückel type tight-binding method in the MO calculation of the dissociative adsorption of diatomic molecules on metal surfaces. In case of CO on Ni(100) and Ni(111) surface,<sup>16,17</sup> they found that the overlap population between the two atoms of carbon monoxide decreases by filling the CO 2 $\pi$  orbital with the *dn* electrons of Ni surface to result in the dissociation of the CO molecule. In a previous paper of authors,<sup>18</sup> the MO calcu-

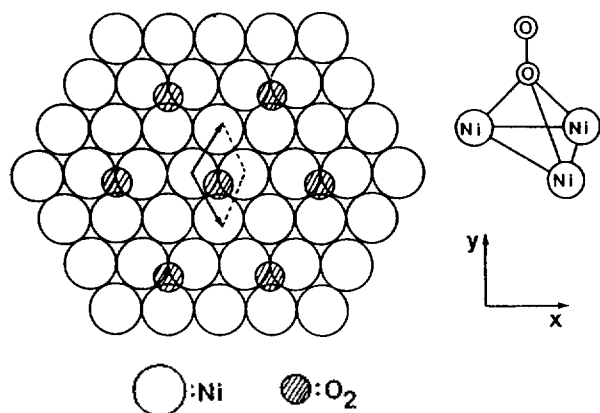


**Table 1.** Interaction between the oxygen molecule and the nickel atoms in the Ni44(111)-p(2×2)O<sub>2</sub> system

neighbors	Interaction energy <sup>a</sup> of Ni and O <sub>2</sub> (kJ/mol)	Overlap population <sup>a</sup> of Ni and O (e)
1st	-106.48	0.05
2nd	1.57	0.00
3rd	0.51	0.00
4th	9.3×10 <sup>-3</sup>	0.00

<sup>a</sup>These are the average values of the interaction with the 1st, 2nd, 3rd and 4th Ni neighbors which contains 3, 3, 6 and 6 atoms, respectively.

**Figure 1.** The Ni44(111) model surface and the vertical adsorption model of oxygen molecules on three-fold sites of the surface.

lation has been made for a system of oxygen molecule interacting with a Ni24(100) model surface to find the dissociative adsorption through the electron transfer from Ni  $d\delta$ , instead of  $d\pi$ , to  $1\pi_g$  of the oxygen molecule. It seems necessary to calculate further with Ni(111) plane in order to see if the  $d\delta$  orbital is solely responsible for the dissociative adsorption of oxygen molecule on the Ni surfaces.

In this work, the interaction of oxygen molecule with the Ni(111) surface to which the molecule approaches, and the dissociation mode are studied by calculating the electron density, the density of state (DOS), and the crystal orbital overlap population (COOP) for the oxygen p(2×2) layer on a Ni44(111) model surface using the extended Hückel type tight-binding method.

## Results

The Ni(111) surface consisting of 44 atoms is taken as the model surface of this work and oxygen molecules are assumed to occupy vertically the three-fold centre<sup>14,19</sup> of this model surface to form p(2×2) layer as shown in Figure 1.

The bond distance between two adjacent nickel atoms and that of oxygen molecule are taken as 24.9 nm<sup>17,20</sup> and 12.1 nm,<sup>21</sup> respectively. The interaction of the oxygen molecule with the three-fold center of the model surface to which the molecule approaches vertically is calculated to investigate the degree of contribution from the different neighboring nickel atoms. It is found that the oxygen molecule interacts mainly with the nearest neighbor nickel atoms which form the three-fold site and hardly with the 2nd nearest neighbor nickel atoms nor the adjacent oxygen molecules as shown in Table 1.

The similar result of the nearest neighbor interaction has been obtained with the Ni24(100) model surface in the previous works of others including authors.<sup>18,22</sup> The result of this nearest neighbor interaction is extended to the unit lattice interaction, assuming that the unit cell simplification will give the same Ni(111) surface properties, relevant to the surface-adsorbate interaction, with those calculated using the whole model surface. The unit cell taken in this work is indicated by two vector arrows in Figure 1. To validate fur-

ther the assumption of the unit cell simplification, the Fermi energy level is calculated in this work with 74 K point set to obtain -9.231 eV. It agrees well with the value, -9.23 eV, calculated recently by Simon *et al.*<sup>23</sup> with Ni605(111) surface using the extended Hückel type method.

The electron density, the DOS, and the COOP are calculated for the adsorption system of the oxygen molecule on the top of the three-fold site of this unit cell as shown in Figure 1. The calculation method and the parameters used are given in the appendix at the end of this work.

**Ni d-DOS.** The Ni d-DOS is calculated with the varying vertical distances of the oxygen molecule from the model surface in order to investigate the Ni d-electron density change upon the adsorption of oxygen onto the nickel surface. From this total DOS of the Ni d-orbital, its constituents,  $d\pi$  ( $d_{xz, yz}$ ),  $d\delta$  ( $d_{x^2-y^2, xy}$ ), and  $d\sigma$  ( $d_{z^2}$ ) are projected out, and the results are shown in Figure 2.

The figure shows that the DOS of Ni  $d\pi$  ( $d_{xz, yz}$ ),  $d\delta$  ( $d_{x^2-y^2, xy}$ ), and  $d\sigma$  ( $d_{z^2}$ ) orbitals shift up gradually above the Fermi level (-9.23 eV) as the oxygen molecule approaches close to the nickel surface. This means that the electron density in these Ni d-orbitals decrease upon the adsorption of oxygen molecule. (Fig. 2(a),  $R_{\perp}=13$  nm). It is noted that the shifts are most prominent in the  $d\pi$ -DOS among the three d-DOS, suggesting that the  $d\pi$  orbital makes a main contribution to the Ni(111)-O<sub>2</sub> interaction. The COOP between two adjacent nickel atoms are calculated with the oxygen molecule separated at three different  $R_{\perp}$ 's above the Ni surface in order to clarify the Ni(111)-O<sub>2</sub> interaction and the results are shown in Figure 3.

It can be seen that the overlap population between the nickel atoms is positive near the Fermi level when the oxygen molecule is infinitely separated from the surface, and it turns gradually into negative as the oxygen molecule approaches close to the surface, suggesting concentrated electrons between the nickel surface and the oxygen molecule.

**Intramolecular bonding of oxygen molecule.** The COOP of the oxygen molecule is calculated with the varying vertical distances above the nickel surface, and the results are shown in Figure 4.

It can be seen that the bonding  $3\sigma_g$  orbital shifts from -15.29 eV to -15.80 eV as the oxygen molecule approaches to the surface as close as to  $R_{\perp}=13$  nm, and the overlap population of antibonding  $1\pi_g$  orbital at -13.0 eV decreases at the same time. These are the result of the weakening

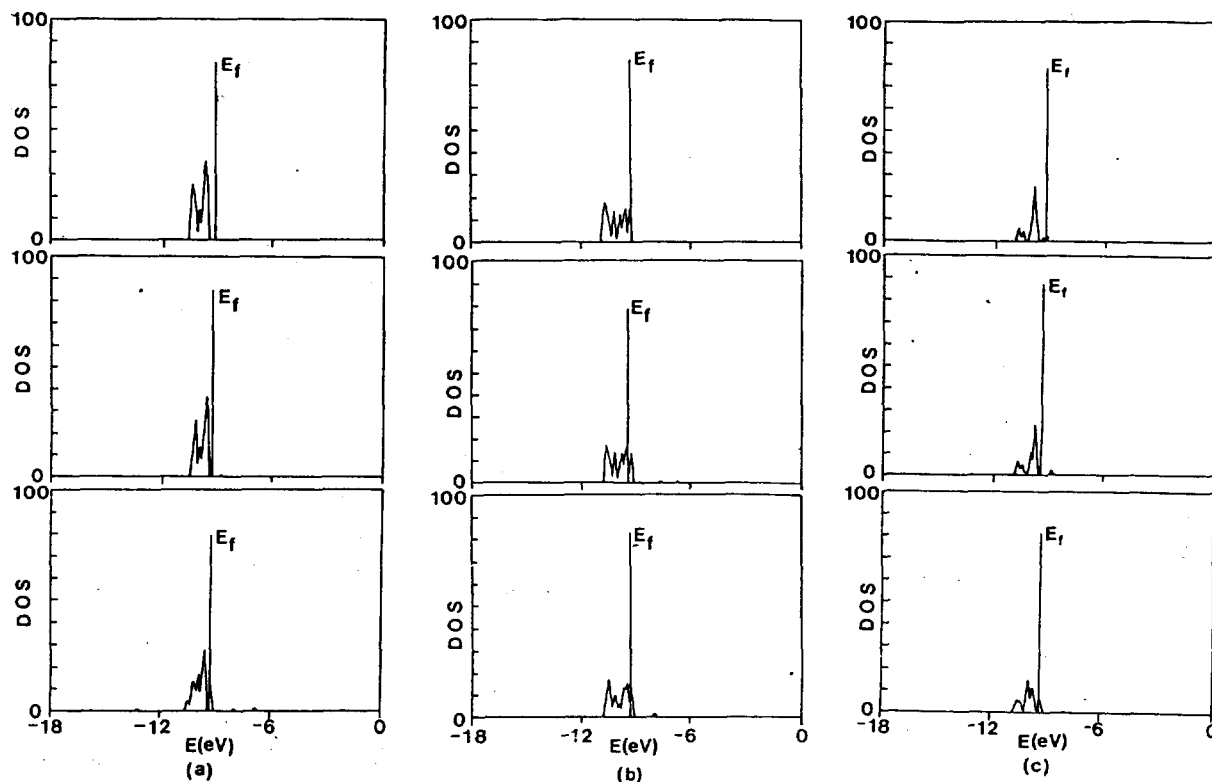


**Figure 2.** Projected d-DOS of Ni: a)  $d\pi$  orbitals; b)  $d\delta$  orbitals, and c)  $d\sigma$  orbital. Each figure consists of three parts corresponding to the vertical distance, from top,  $R_{\perp}$ , of infinity, 20 nm, and 13 nm, respectively.

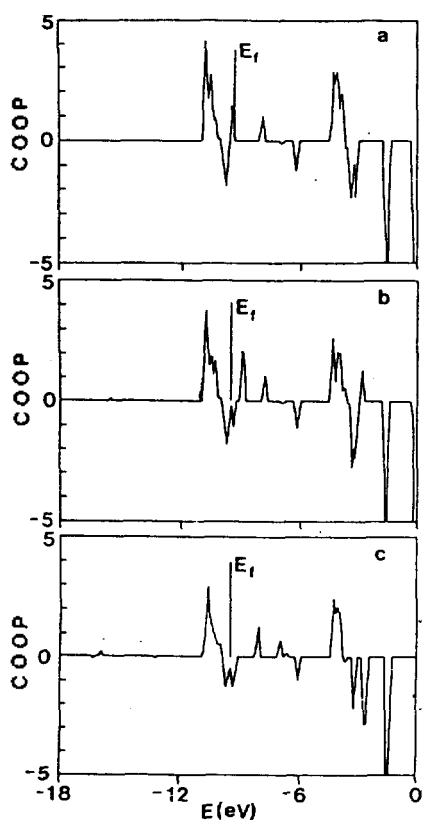


**Figure 3.** COOP of Ni-Ni with oxygen molecule at  $R_{\perp}$  of a)  $\infty$ , b) 20 nm, and c) 13 nm.

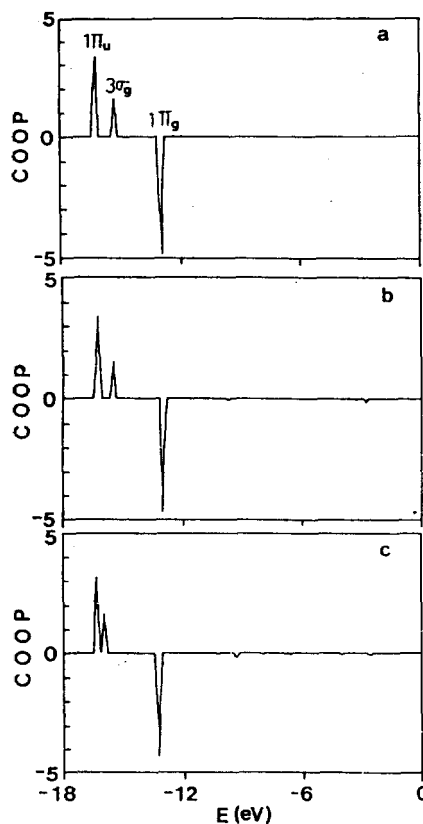


**Figure 4.** Projected COOP of O-O bond when the  $R_{\perp}$  is equal to a)  $\infty$ , b) 20 nm, and c) 13 nm.

**Table 2.** Electronic structure of the oxygen and Ni(111) surface

Electron density with $R_{\perp} = \infty$							
O <sub>2</sub>			Ni(111) surface				
$3\sigma_g$	$1\pi_u$	$1\pi_g$	$d\sigma$	$d\pi$	$d\delta$	total	$E_F$ (eV)
2.00	4.00	2.00	1.98	4.00	3.39	9.37	-9.23
Electron density with $R_{\perp} = 13$ nm							
$3\sigma_g$	$1\pi_u$	$1\pi_g$	$d\sigma$	$d\pi$	$d\delta$	total	$E_F$ (eV)
1.81	3.89	3.55	1.92	3.82	3.48	9.22	-9.26
Electron density change upon adsorption							
$\Delta 3\sigma_g$	$\Delta 1\pi_u$	$\Delta 1\pi_g$	$\Delta d\sigma$	$\Delta d\pi$	$\Delta d\delta$	$\Delta$ total	$\Delta E_F$ (eV)
-0.19	-0.11	1.55 <sup>a</sup>	-0.06	-0.18	0.09	-0.15	-0.03
Overlap population							
Ni-O			O-O				
$R_{\perp} = \infty$	0.00		0.77				
$R_{\perp} = 13$ nm	0.10		0.47				

<sup>a</sup>The electron density of  $1\pi_g$  is for the two degenerate  $1\pi_g$  orbitals, which means 0.78e for each.

of the O-O bond strength.  $R_{\perp} = 13$  nm corresponds to 19.4 nm of Ni-O distance<sup>14</sup> when the oxygen molecule occupies the three-fold site of Ni(111) surface at equilibrium.

#### Dissociation of oxygen molecule on adsorption.

As the changes in electron densities and overlap populations of Ni  $d\pi$ , and O<sub>2</sub>  $1\pi_g$  orbitals are shown as the main cause of the interaction between the oxygen molecule and Ni(111) surfaces, their magnitude and the relevant overlap population between the nickel and oxygen atoms are calculated with  $R_{\perp} = 13$  nm to investigate the interaction in terms of the frontier orbitals, and the results are shown in Table 2.

According to the table, the electron density of the bonding  $3\sigma_g$  and  $1\pi_u$  orbitals of the oxygen molecule decreases by 0.19e and 0.11e, respectively, while that of the antibonding  $1\pi_g$  orbitals increases by 0.78e each as the molecule is adsorbed on the nickel surface. Meanwhile, the electron density of Ni  $d$  orbitals decreases as a whole. However, the decrease is most prominent in Ni  $d\pi$  ( $d_{xz, yz}$ ) orbitals. The overlap population between the Ni(111) surface and the oxygen atom, calculated in this work, increases by 0.10e, while the overlap population between two oxygen atoms decreases by 61% from 0.77e to 0.47e upon the adsorption.

The DOS of the oxygen molecule and Ni  $d\pi$  orbitals, and the COOP between the nickel surface and the oxygen atom calculated in this work are shown in Figure 5.

The figure shows that the Ni  $d\pi$  orbital and the O<sub>2</sub>  $1\pi_g$  orbital interact at -13.1 eV and -6.9 eV, and the overlap population between the nickel surface and the oxygen atom is positive at -13.1 eV, while it is negative at -6.9 eV. Thus the interaction is bonding at -13.1 eV, while it is antibonding at -6.9 eV. These bonding and antibonding interactions can be explained in terms of the bonding overlap and the antibonding overlap schemes as shown below.

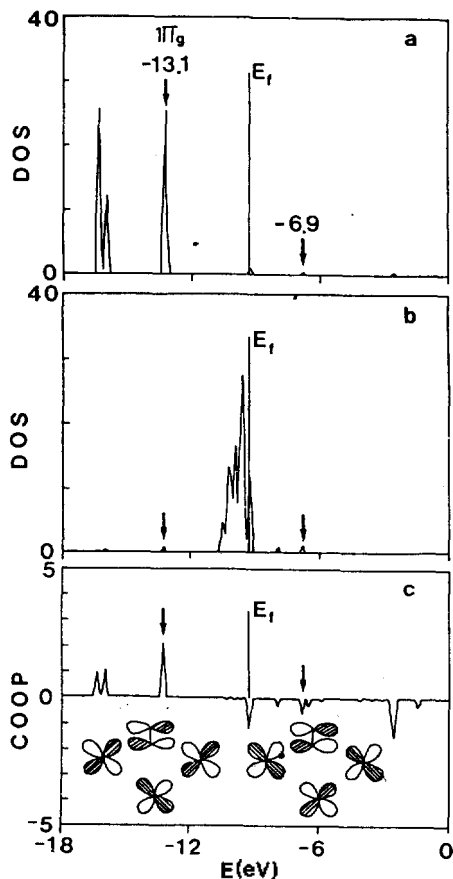
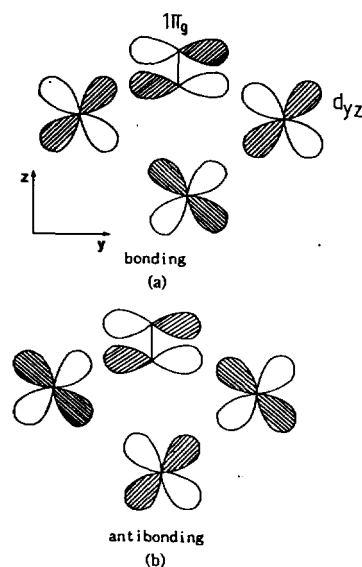


**Figure 5.** a) The total-DOS of O<sub>2</sub>, b) the  $d\pi$  DOS of Ni, and c) the COOP of Ni-O; at  $R_{\perp} = 13$  nm.



**Scheme 1.**

In conclusion, in case oxygen molecule adsorbs on the Ni(111) surface, the Ni-O bond is formed through the electron transfer from the Ni  $d\pi$  orbital into the antibonding  $1\pi_g$  orbital of the oxygen molecule. This is contrasted with the electron transfer from Ni  $d\delta$  into O<sub>2</sub>  $1\pi_g$  orbitals in case the molecule adsorbs on the Ni(100) surface.

**Table 3.** EHT parameters used in this calculation

	$\zeta_{ms}$	$H_{ms}$	$\zeta_{mp}$	$H_{mp}$	$\zeta_{md1}$	$H_{md}$	$C_1^*$	$\zeta_{md2}$	$C_2^*$
Ni	2.100	-7.80	2.100	-3.70	5.750	-9.90	0.5683	2.00	0.6292
O	2.275	-32.30	2.275	-14.80					

\*coefficient of double expansion

**Acknowledgment.** This work is supported financially by the Ministry of Education, through the Basic Research Institute program.

### Appendix

The calculations are made with the tight-binding EHT method using PC/386 and PC/486. The QCPE 571 (VAX version)<sup>24</sup> is converted into the MS-Fortran version<sup>18</sup> and this program is compiled by MS-Fortran version 5.0 under OS/2 version 1.1. The parameters used in this calculation are, by the charge interaction method due to Hoffmann, shown in Table 3.

### References

- Shayegan, M.; Cavallo, J. M.; Glover, R. E.; Park, R. L. *Phys. Rev. Lett.* **1984**, *53*, 1578.
- Ham, K. H.; Ahn, W. S. *Bull. Kor. Chem. Soc.* **1990**, *11*, 231.
- Beckerle, J. D.; Yang, Q. Y.; Johnson, A. D.; Geyer, S. T. *Surf. Sci.* **1988**, *195*, 77.
- Park, P. L.; Fransworth, H. E. *Appl. Phys. Lett.* **1963**, *3*, 167.
- Fransworth, H. E. *Appl. Phys. Lett.* **1963**, *2*, 199.
- Demuth, J. E.; Rhodin, T. N. *Surf. Sci.* **1974**, *45*, 249.
- Holloway, P. H.; Hudson, J. B. *Surf. Sci.* **1974**, *43*, 123.
- Conrad, H.; Ertl, G.; Küppers, J.; Latta, E. E. *Surf. Sci.* **1976**, *57*, 475.
- Norton, P. R.; Toppind, R. L.; Goodale, J. W. *Surf. Sci.* **1977**, *65*, 13.
- Dolle, P.; Tommasini, M.; Jupille, J. *Surf. Sci.* **1989**, *211/212*, 904.
- Altmann, W.; Desiger, K.; Donath, M.; Dose, V.; Goldmann, A.; Scheidt, H. *Surf. Sci.* **1985**, *151*, L185.
- Caputi, L. S.; Jiang, S. L.; Tucci, R.; Amoddeo, A.; Pagnano, L. *Surf. Sci.* **1989**, *211/212*, 120.
- Lee, S. B.; Boo, J. H.; Ham, K. H.; Ahn, W. S.; Lee, K. S. *Bull. Kor. Chem. Soc.* **1988**, *9*, 32.
- Marcus, P. M.; Demuth, J. E.; Jepsen, D. W. *Surf. Sci.* **1975**, *53*, 501.
- Saillard, J. Y.; Hoffmann, R. *J. Am. Chem. Soc.* **1984**, *106*, 2006.
- Sung, S. S.; Hoffmann, R. *J. Am. Chem. Soc.* **1985**, *107*, 578.
- Wong, Y. T.; Hoffmann, R. *J. Phys. Chem.* **1991**, *95*, 859.
- Lee, K. S.; Koo, H. J.; Park, Y. C.; Ahn, W. S. *Bull. Kor. Chem. Soc.* **1994**, *15*, 139.
- Hock, M.; Küppers, J. *Surf. Sci.* **1987**, *188*, 575.
- Germer, L. H.; Hartman, C. D. *J. App. Phys.* **1960**, *31*, 2085.
- Wells, A. F. *Structural Inorganic Chemistry*; Clarendon Press: Oxford, 1984, p 498.
- Rhamann, T. S.; Black, J. E.; Mills, D. L. *Phys. Rev. Lett.* **1981**, *46*, 1469.
- Simon, D.; Bigot, B. *Surf. Sci.* **1994**, *306*, 459.
- Whangbo, M. H.; Evain, M.; Hughbanks, T.; Kertesz, M.; Wijeyesekera, S.; Wilker, C.; Zheng, C.; Hoffmann, R. EHMCC(QCPE 571), *QCPE Bull.* **1989**, *9*, 61.